Drosophila kinesin-8 stabilises kinetochore-microtubule interaction

Tomoya Edzuka and Gohta Goshima[#]

Division of Biological Science, Graduate School of Science, Nagoya University, Furo-cho, Chikusa-ku, Nagoya 464-8602, Japan, [#] goshima@bio.nagoya-u.ac.jp

Kinesin-8 is required for proper chromosome alignment in a variety of animal and yeast cell types. However, how this conserved motor protein controls chromosome alignment remains unclear, as multiple biochemical activities, including inconsistent ones between studies, have been identified for this motor family. Here, we show that *Drosophila* kinesin-8 Klp67A possesses both microtubule (MT) plus-end-stabilising and -destabilising activities in addition to commonly observed MT plus-end-directed motility and tubulin-binding activity *in vitro*, and is required for stable kinetochore-MT attachment during prometaphase *in vivo*. In the absence of kinesin-8^{Klp67A}, abnormally-long MTs interact in an "end-on" fashion with kinetochores at normal frequency. However, the interaction was not stable and, once-attached, MTs were frequently detached. This phenotype was rescued by ectopic expression of MT plus-end-stabilising factor CLASP, but not by artificial shortening of MTs. These results suggest that MT-stabilising activity of kinesin-8^{Klp67A} is critical for stable kinetochore-MT attachment.

Introduction

Equal segregation of sister chromatids into daughter cells relies on proper attachment of microtubules (MTs) to a specialised site on the chromosome, the kinetochore. Kinetochores consist of dozens of proteins, including those that bind to DNA or MTs, and many of them form subcomplexes for normal function (Musacchio and Desai, 2017). The Ndc80 complex is localised to the kinetochore during mitosis and functions as the major MT attachment site: "end-on" attachment of MTs to kinetochores absolutely depends on this conserved protein complex (Cheeseman et al., 2006; Powers et al., 2009; Musacchio and Desai, 2017). In yeast and animals, the Dam1 and Ska1 complexes, respectively, support MT binding of the Ndc80 complex (Tien et al., 2010; Schmidt et al., 2012). However, these complexes might not be the sole critical factors for MT attachment, as other MT-associated proteins, such as motor proteins, are also enriched at the kinetochore (Musacchio and Desai, 2017).

Besides attachment, kinetochores regulate the dynamics of the associated MTs. A major regulator is cytoplasmic linker associated protein (CLASP), which promotes persistent growth of kinetochore MTs (Maiato et al., 2003; Maiato et al., 2005). In its absence, MTs continuously shrink and spindles collapse (Maiato et al., 2005). *In vitro*, CLASP retards MT growth and acts as a potent inhibitor of MT "catastrophe" and as an inducer of "rescue" (Al-Bassam et al., 2010; Moriwaki and Goshima, 2016; Yu et al., 2016). Another key regulator of kinetochore MT dynamics is the kinesin-8 motor protein.

Kinesin-8 is widely conserved kinesin subfamily and possesses its motor domain at the N-terminus, followed by coiled-coil and tail regions. Mitotic functions of kinesin-8 have been well described for budding yeast Kip3 (Cottingham and Hoyt, 1997; Straight et al., 1998; Tytell and Sorger, 2006; Wargacki et al., 2010), fission yeast Klp5/Klp6 (Garcia et al., 2001; West et al., 2002), *Drosophila* Klp67A (Goshima and Vale, 2003; Gandhi et al., 2004; Savoian et al., 2004; Savoian and Glover, 2010), and mammalian KIF18A (Mayr et al., 2007; Stumpff et al., 2008) and KIF18B (McHugh et al., 2018). Kinesin-8 is generally enriched at the outer region of the mitotic kinetochore, where plus ends of

kinetochore MTs are present, and its depletion affects spindle length and chromosome alignment. In human KIF18A RNAi, the amplitude of chromosome oscillation in the abnormally-elongated spindle is dramatically elevated, such that chromosome congression cannot be achieved. In the absence of budding yeast Kip3, kinetochores are unclustered in the spindle, indicating chromosome alignment defects. Fission yeast klp5/6 mutant also exhibited chromosome misalignment associated with Mad2-dependent mitotic delay. Overall, loss of kinesin-8 consistently perturbs chromosome alignment in a variety of cell types.

Despite the conserved phenotype and localisation associated with kinesin-8, its biochemical activity towards MTs is inconsistent between reports. The best-studied budding yeast Kip3 has plus-end-directed, processive motility and also has strong MT depolymerising activity; it can depolymerise MTs stabilised by GMPCPP (non-hydrolysable GTP) and promote catastrophe (growth-to-shrinkage transition) in dynamic MTs (Gupta et al., 2006; Varga et al., 2006). The C-terminal tail has MT- and tubulin-binding activities, which allows this motor to crosslink and slide antiparallel MTs (Su et al., 2011; Su et al., 2013). However, MT depolymerisation activity has not been detected for fission yeast proteins Klp5/Klp6 and, instead, MT nucleation activity has been reported (Erent et al., 2012). Humans have two mitotic kinesin-8s, KIF18A and KIF18B, and the kinetochore function has been observed for KIF18A. KIF18A, like Kip3, exhibits processive motility towards plus ends, and accumulates at the plus end on its own (Mayr et al., 2007; Du et al., 2010). The tail region of KIF18A has MT and tubulin affinity, which is similar to Kip3 (Mayr et al., 2011; Weaver et al., 2011). However, its impact on MT dynamics has been controversial. In one study, KIF18A was concluded to have MT depolymerising activity, based on its depolymerisation activity towards stabilised MTs (Mayr et al., 2007). In another study, however, this activity was reported to be undetectable, and instead, it dampened MT dynamicity; KIF18A suppressed both growth and shrinkage of MTs (Du et al., 2010). Although the former activity is more consistent with Kip3, the latter activity appears to be more congruous with the cellular phenotype associated with KIF18A (Stumpff et al., 2008).

In the present study, we investigated Klp67A, the sole mitotic kinesin-8 in *Drosophila*. In addition to conserved MT-based motility, we identified both MT stabilising and destabilising activities in a single experimental condition. Functional analysis in the S2 cell line indicated that, with these two activities, kinesin-8^{Klp67A} not only regulates MT length, but also stabilises kinetochore-MT attachment.

Results

Kinesin-8^{Klp67A} shows plus-end-directed motility and tubulin-binding activity *in vitro*

Generally observed biochemical activities among mitotic kinesin-8 motors are processive motility (Gupta et al., 2006; Varga et al., 2006; Stumpff et al., 2011; McHugh et al., 2018) and tubulin binding at the non-motor region (Mayr et al., 2011; Su et al., 2011; Weaver et al., 2011). To determine the biochemical activity of *Drosophila* kinesin-8^{Klp67A}, we purified recombinant GFP-tagged full-length protein (Fig. 1A). First, we performed single motor motility assays and found that kinesin-8^{Klp67A}-GFP is a processive motor with approximate velocity 25 ± 0.7 μm/min (mean ± SE) (Fig. 1B, C). The GFP signal accumulated at one end of MTs (Fig. 1B). Next, we determined the directionality by localising kinesin-8^{Klp67A}-GFP on the MTs that underwent gliding by the plus-end-directed kinesin-1 motor (Fig. 1D). Kinesin-8^{Klp67A}-GFP was enriched at the trailing end of MTs, indicating that kinesin-8^{Klp67A} is a plus-end-directed motor, as seen with other kinesin-8s (Fig. 1E).

Kinesin-8^{Klp67A} was also localised along the stabilised MT seed that was prepared with GMPCPP. We observed that free tubulin, which was labelled with a different colour from that of kinesin-8^{Klp67A} or MT seed, was

recruited to the MT seed by kinesin-8^{Klp67A}, indicating the tubulin-binding activity of kinesin-8^{Klp67A} (Fig. 1F, G, Fig. S1).

Kinesin-8^{Klp67A} has both MT-destabilising and -stabilising activities *in vitro*

We next determined the effect of kinesin-8^{Klp67A} on MT polymerisation dynamics in an *in vitro* assay (Fig. 2A). When we mixed 5, 10, 20, or 50 nM kinesin-8^{Klp67A} with GMPCPP-stabilised MT seeds and free tubulin (10 μM), dynamic MTs from the seeds were rarely or never observed at 20 nM or 50 nM, respectively (Fig. 2B). Therefore, we quantified the dynamics parameters in the presence of 5 or 10 nM kinesin-8^{Klp67A} (Fig. 2C–G). As expected from the spindle lengthening phenotype, kinesin-8^{Klp67A} elevated the catastrophe frequency of the MTs. The growth rate was slightly increased, which was consistent with a recent report concerning human kinesin-8^{KIF18B} (McHugh et al., 2018). Interestingly, kinesin-8^{Klp67A} also increased the rescue frequency and slowed down shrinkage under the same assay conditions, which resulted in more frequent pausing (Fig. 2H). Thus, we observed both MT-stabilising and -destabilising effects reported for kinesin-8^{KIF18A} by (Du et al., 2010) and (Mayr et al., 2007; Locke et al., 2017), respectively. However, we did not observe MT depolymerisation activity of kinesin-8^{Klp67A} towards GMPCPP-stabilised MTs at this motor concentration, which differs from that for yeast Kip3 (Gupta et al., 2006; Varga et al., 2006), human KIF18A reported by (Mayr et al., 2007; Locke et al., 2017), or the bona fide MT-depolymerising *Drosophila* kinesin-13^{Klp10A} (Rogers et al., 2004) that was used as a positive control in our experiments (Fig. 2I).

Kinesin-8^{Klp67A} depletion causes instability of kinetochore-MT attachment

To explore the function of kinesin-8^{Klp67A} in the spindle, we observed the RNAi phenotype in living S2 cells. In addition to chromosomes and MTs, we traced GFP-Rod: GFP-Rod accumulates at unattached kinetochores and, once MTs are attached in an end-on fashion, it is transported away from the kinetochore along the MTs (Basto et al., 2004; Gluszek et al., 2015). Therefore, GFP-Rod exhibits “flux” upon MT end-on attachment, while residual proteins are still visible at the kinetochore; thus, it serves as an ideal marker for kinetochore dynamics as well as for its attachment status (Fig. 3A). To precisely monitor and evaluate the dynamics of individual chromosome and GFP-Rod signals in the uniformly-shaped spindle, we induced monopolar spindles by depleting Klp61F, the kinesin-5 motor protein required for spindle bipolarisation. In control cells that were singly depleted of kinesin-5^{Klp61F}, we observed that the majority of sister kinetochores were attached to MTs from the pole (“syntelic” attachment), with weak GFP-Rod signals detected (Fig. 3B, Movie 1). The syntelically-attached kinetochores were static and scarcely changed position during the observation time. In some instances, we observed “monotelic” attachment at the beginning, where one of the sister kinetochores was not associated with MTs and, therefore, a strong GFP-Rod signal was detected (Fig. 3C, 12 s). However, they were converted into syntelic attachments during imaging, which was characterised by GFP-Rod flux along the newly formed kinetochore MTs (Fig. 3C, 153 s). Once syntelic attachment was established, MTs were rarely dissociated from kinetochores (Fig. 3D, control).

When kinesin-5^{Klp61F} and kinesin-8^{Klp67A} were co-depleted, monopolar spindles with much longer MTs were assembled, as reported (Fig. 3B)(Goshima and Vale, 2003). In addition, kinetochore dynamics were dramatically different in such depleted cells (Movie 1). Some kinetochores were visibly motile, and monotelic attachment was more frequently observed for those chromosomes. Most of the unattached kinetochores acquired end-on attachment during the imaging period, as indicated by GFP-Rod flux (e.g. Fig. 3C, 171-174 s), although the associations were often transient. Quantification indicated detachment of MTs

from the kinetochore was significantly more frequently observed in the absence of kinesin-8^{Klp67A}, whereas the end-on attachment event was detected at a similar frequency to that in control cells (Fig. 3D, E). Interestingly, MT detachment was usually associated with chromosome flipping, where a sister kinetochore initially located remote from the pole was flipped and faced the pole (e.g. Fig. 3C, 89–387 s). These data indicated that kinetochores are able to bind to MTs but that this attachment is unstable in the monopolar spindle without kinesin-8^{Klp67A}.

We next observed GFP-Rod behaviour in the bipolar spindle with or without kinesin-8^{Klp67A} (Fig. 4). As previously reported, abnormally-elongated spindles with unaligned chromosomes were observed without kinesin-8^{Klp67A}. Since MTs were crowded in the spindle, it was impossible to observe MT attachment status for most kinetochores. Nevertheless, when we focused on completely unaligned chromosomes that are remote from the main body of the spindle, we observed a similar phenotype to that observed in the monopolar assay. In the control cell displayed in Fig. 4A and Movie 2, a chromosome (arrow) was not immediately captured by MTs and remained near the pole; it had strong GFP-Rod signals. However, MTs were generated independent of centrosomes and bound to the kinetochore (63 s). Once those MTs are formed, flow of GFP-Rod was visible, concomitant with the decrease of the kinetochore signal intensity (93–180 s). Thus, a bi-oriented chromosome with “amphitelic” attachment was finally observed, and it was translocated towards the spindle equator (375 s). In contrast, MT attachment was unstable and MT detachment was observed in kinesin-8^{Klp67A}-depleted cells. In the case displayed in Fig. 4B and Movie 2, a misaligned chromosome (arrow) achieved amphitelic attachment at 114 s, as evident by GFP-Rod flux along chromosome-bound MTs, but then such a configuration was disrupted at 198 s and the chromosome was flipped (198–285 s).

From these results, we concluded that the MT-kinetochore association becomes unstable in the absence of kinesin-8^{Klp67A}.

Artificial MT destabilisation does not rescue the kinesin-8^{Klp67A}-depleted phenotype

Attachment instability might be the consequence of longer MTs in the absence of kinesin-8^{Klp67A}. To test this possibility, we depleted kinesin-5^{Klp61F} and Dgt6, an essential subunit of the MT amplifier augmin, to generate monopolar spindles with long MTs; MTs are elongated in this condition due to the reduction of MT nucleation sites within the spindle (Goshima et al., 2008). Augmin^{Dgt6}/kinesin-5^{Klp61F} RNAi-treated cells indeed exhibited much longer and pendulous MTs, similar to those observed after kinesin-8^{Klp67A} depletion (Fig. S2A, Movie 3). Monotelic and syntelic attachments were both observed, similar to that seen in kinesin-8^{Klp67A}-depleted cells. However, once-attached, MTs were more persistent and chromosome flipping was rarely observed (Fig. 5D).

To further exclude the possibility that abnormally-elongated MTs due to reduced catastrophe are the major cause of MT attachment instability, we exposed a low dosage of colcemid to kinesin-8^{Klp67A} RNAi-treated cells and shortened the bipolar spindle lengths to the control levels (Fig. S2B, C). Unaligned chromosomes were still frequently observed and mitosis was significantly delayed (Fig. S2B, D). These results suggested that regulation of MT length alone cannot explain the attachment instability of kinesin-8^{Klp67A}-depleted cells.

Aurora B kinase inhibition or CLASP$^{Mast/Orbit}$ overexpression rescues attachment instability caused by kinesin-8^{Klp67A} depletion

In mammalian cells, inhibition of Aurora B kinase stabilises syntelic attachment, due at least in part to dephosphorylation of Ndc80: Ndc80 is a critical kinetochore component for MT binding and the MT binding affinity is decreased by Aurora B

phosphorylation (Cheeseman et al., 2002; DeLuca et al., 2006; Lampson and Grishchuk, 2017; Musacchio and Desai, 2017). We added the inhibitor of *Drosophila* Aurora-B, Binucleine-2 (Smurnyy et al., 2010), to S2 cells depleted of kinesin-8^{Klp67A}/kinesin-5^{Klp61F}, and observed that most kinetochores stably attached MTs in a syntelic manner, as indicated by a decrease in GFP-Rod signals (Fig. 5A, Movie 4). The result indicates that kinetochores retain an ability to bind stably to MTs in the absence of kinesin-8^{Klp67A}, when Aurora B activity is low. Our interpretation is that the MT-binding potential of the dephosphorylated form of Ndc80 complexes is preserved in the absence of kinesin-8^{Klp67A}.

In the absence of kinesin-8^{Klp67A}, persistent poleward motility of chromosomes was observed, which would involve kinetochore MT shrinkage (Movie 1). We hypothesised that the MT stabilisation activity of kinesin-8^{Klp67A}, namely slowing down MT shrinkage and inducing rescue/pausing, is critical for MT attachment stability. If that were the case, we reasoned that MT stabilisation by other means might partially suppress the MT detachment phenotype. To this end, we expressed *Drosophila* CLASP (also called Mast or Orbit) in kinesin-8^{Klp67A}/kinesin-5^{Klp61F} RNAi cells and observed the consequent chromosome dynamics. Since we attached GFP to CLASP$^{Mast/Orbit}$ to identify cells overexpressing CLASP$^{Mast/Orbit}$, GFP-Rod signals could not be used to evaluate MT-kinetochore attachment status. Nevertheless, chromosome flipping frequency was significantly reduced in GFP-CLASP$^{Mast/Orbit}$ overexpressing cells, supporting our hypothesis (Fig. 5B–D, Movie 5).

Discussion

Biochemical activity of kinesin-8^{Klp67A}

We observed processive plus-end-directed motility, catastrophe-induction, and rescue/pausing activity of kinesin-8^{Klp67A} towards MTs. This combination of activities has not been observed for another five *Drosophila* MT plus-end-regulating proteins we have characterised so far using an identical assay (Li et al., 2012; Moriwaki and Goshima, 2016). Motility and catastrophe induction can be deduced from the amino acid sequences of Klp67A's motor domain. In contrast, how rescue/pausing activity is executed remains unclear; it might involve the tubulin-binding region in the tail to increase the local concentration of tubulin.

Whether human KIF18A is a depolymerase (Mayr et al., 2007; Locke et al., 2017) or MT dynamics suppressor (Du et al., 2010) has been debated. However, those studies used distinct assay and buffer conditions *in vitro*; it is possible that KIF18A can execute both activities in cells, namely, being endowed with a similar set of activities to *Drosophila* Klp67A. Budding yeast Kip3 is an established MT depolymerase, but rescue and pausing frequencies are also reduced in the mutant *in vivo* (Gupta et al., 2006), for which the tubulin-binding region is involved (Su et al., 2011). Our study suggests that the multiple activities observed here for kinesin-8^{Klp67A} in a single experimental condition are widely conserved among kinetochore-localised kinesin-8s.

Kinesin-8^{Klp67A} is required for stable kinetochore-MT attachment

Previous studies using RNAi or mutants of kinesin-8^{Klp67A} consistently reveal its role in spindle length regulation (Goshima and Vale, 2003; Savoian et al., 2004; Gatt et al., 2005; Goshima and Vale, 2005; Goshima et al., 2005; Buster et al., 2007; Wang et al., 2010). This was confirmed in this study, and most likely is attributed to the catastrophe-inducing function. However, experiments involving colcemid treatment indicated that MT elongation with reduced catastrophe is not the causal factor leading to chromosome misalignment. GFP-Rod imaging further uncovered a specific role of kinesin-8^{Klp67A} at the kinetochore-MT interface: it ensures persistent MT attachment to the kinetochore.

Why are MTs frequently detached in the absence of kinesin-8^{Klp67A}? We observed that overexpression of the MT rescue/pausing

factor CLASP largely rescued the flipping behaviour of chromosomes. Since flipping is associated with the detachment event, we interpret that CLASP overexpression reduced MT detachment rates. The data therefore suggest that kinetochores are prone to detach from MTs during rapid and persistent depolymerisation. On the other hand, *in vitro* study using Ndc80-decorated beads and depolymerising MTs indicated robust load-bearing attachment of the beads during depolymerisation (Powers et al., 2009). However, this observation might be reconciled with our findings, as Aurora B kinase could dampen Ndc80's MT binding ability *in vivo*. Consistent with this notion, we observed stable MT association when Aurora B kinase was inhibited. We propose that kinesin-8^{Klp67A} constitutes an additional layer of the MT attachment interface.

Re-interpretation of the human KIF18A depletion phenotype

It was previously reported that KIF18A depletion increases the amplitude of chromosome oscillation, where MT dynamics regulation, rather than attachment per se, is defective (Stumpff et al., 2008). This behaviour is consistent with the *in vitro* MT stabilisation activity (Du et al., 2010). However, a more recent study demonstrated that kinetochore-MT interaction is also perturbed in this condition (Kim and Stumpff, 2018), which is actually more consistent with a fixed cell study that shows the presence of Mad2-positive chromosomes (Mayr et al., 2007). The study attributes the phenotype partly to defects in KIF18A-dependent PP1 delocalisation (Kim and Stumpff, 2018); however, those investigations also showed the presence of a PP1-independent function of KIF18A for chromosome alignment. The PP1-binding motif is not conserved in *Drosophila* Klp67A (De Wever et al., 2014), and therefore PP1 mis-localisation is unlikely to be the primary cause of chromosome misalignment in the absence of kinesin-8^{Klp67A} in S2 cells. Studies in human cells, including our own efforts (unpublished), did not follow the kinetochore-MT attachment status at such high resolution as we achieved in S2 cells. Nevertheless, it is tempting to speculate that the MT shrinkage-suppressing activity is required for stable MT attachment, as we observed in S2 cells. However, KIF18A and Klp67A also have several distinct properties. For example, although Klp67A autonomously localises to the kinetochore, KIF18A requires kinetochore-bound MTs for kinetochore accumulation (Mayr et al., 2007; Savoian and Glover, 2010). Several studies suggest an involvement of KIF18A in carcinogenesis (Zhang et al., 2010; Hitti et al., 2016). It is of interest if KIF18A plays a role in MT attachment stability in an identical manner to *Drosophila* Klp67A in cancer cell models.

Materials and methods

RNAi and cell line selection

Cell culture and RNAi were performed as previously described (Goshima et al., 2007; Bettencourt-Dias and Goshima, 2009; Ito and Goshima, 2015). In brief, Schneider's medium (Gibco) supplemented with 10% serum was used for cell culture. Cell lines were selected with hygromycin or puromycin following plasmid transformation with the TransIT-Insect reagent (Takara). Plasmids used in this study are listed in Table S1, whereas dsRNA sequences employed here are available at (Goshima et al., 2007). For RNAi experiments, cells were treated with dsRNAs for 3–4 days and then plated on concanavalinA-coated glass-bottom dishes for microscopy.

Microscopy

Live imaging was performed with a spinning-disc confocal microscope (Nikon Ti; 100× 1.45 NA or 60 × 1.40 NA lens, EMCCD camera ImagEM [Hamamatsu], CSU-X1 [Yokogawa]). A TIRF microscope was used in the *in vitro* MT dynamics experiment (Nikon Ti; 100× 1.49 NA lens, EMCCD camera Evolve [Roper]). 488/561/640-nm excitation lasers were associated with both microscopes. Microscopes were controlled by micromanager and images were processed with ImageJ. All imaging was performed at approximately 25°C.

Protein purification

S2 tubulin was purified by using a previously described method, using GST-tagged TOG1 domain (*S. cerevisiae* Stu2, 1–306 a.a.) (Widlund et al., 2012; Moriwaki and Goshima, 2016). Klp67A-GFP-6His was expressed in *E. coli* SoluBL21 cells (250 mL culture in L-rich medium, 0.1–0.5 mM IPTG at 18°C for 16–20 h). Cells were resuspended in Lysis Buffer (50 mM MOPS-NaOH [pH = 7.2], 250 mM NaCl, 2 mM $MgCl_2$, 1 mM EGTA, 0.5 mM Phenylmethylsulfonyl fluoride (PMSF), peptide cocktail, 2 mM 2-mercaptoethanol, 0.1 mM ATP), sonicated with a homogeniser (Branson, 450DA), bound to Ni-NTA (4˚C, 60–90 min), washed with Wash Buffer (Lysis Buffer supplemented with 20 mM imidazole and 0.2 % Tween), followed by elution 5–8 times with Elution Buffer (MRB80 [80 mM PIPES-KOH (pH = 6.8), 1 mM EGTA, 4 mM $MgCl_2$], 100 mM KCl, 250 mM imidazole, 2 mM 2-mercaptoethanol, 1 mM ATP). The eluate was subjected to sucrose gradient sedimentation. A 2.5- 40 % sucrose gradient was made with 2 mL buffer (MRB80, 100 mM KCl, 0.1 mM ATP, sucrose) in a 2.2 mL, 11 × 35 mm ultracentrifugation tube (Beckman Coulter, # 347357). Protein solution (200 µL) was applied and centrifuged with a TLS-55 rotor (214,000 × g, 4 h, 4ºC), and 16 fractions were collected. Fractions containing Klp67A-GFP-6His were identified with SDS-PAGE and Coomassie staining, followed by flash freezing. His-Klp10A was purified with Ni-NTA, as previously described (Moriwaki and Goshima, 2016).

In vitro MT polymerisation assay

The *in vitro* MT polymerisation assay was performed essentially following a method previously described (Li et al., 2012; Moriwaki and Goshima, 2016). A silanized coverslip was coated with anti-biotin (1–5% in 1 × MRB80, Invitrogen), and the nonspecific surface was blocked with Pluronic F127 (1% in 1 × MRB80, Invitrogen). Biotinylated MT seeds (50–100 µM tubulin mix containing 10% biotinylated pig tubulin and 10% Alexa647-labelled pig tubulin with 1 mM GMPCPP) were specifically attached to the functionalised surface by biotinylated tubulin-anti-biotin links. After the chamber was washed with 1 × MRB80, MT growth was initiated by flowing 10 µM tubulin (containing 80% S2 tubulin and 20% Alexa568-labelled pig tubulin) and Klp67A-GFP into the assay buffer (1 × MRB80, 75 mM KCl, 1 mM GTP, 1mM ATP, 0.5 mg/mL k-casein and 0.1% methylcellulose, 5.5 % sucrose), and an oxygen scavenger system (50 mM glucose, 400 µg/mL glucose-oxidase, 200 µg/mL catalase, and 4 mM DTT). The samples were sealed with candle wax. During experiments, the samples were maintained at approximately 25°C, and images were collected every 3 s for 15 min using TIRF microscopy. MT depolymerisation assay was conducted in an identical condition, except that no tubulin was included. MT gliding assay was performed following a previous report (Miki et al., 2015) with slight modification to the buffer. Briefly, the flow chamber was washed with 1 × MRB80 and purified kinesin-1 motor (K560-6His) was flowed into the chamber. After washing with MRB80 containing 0.5 mg/ml k-casein, the motility buffer (1× MRB80, 75 mM KCl, GMPCPP-stabilized MTs with Alexa 647-labels, 1 mM ATP, 0.5 mg/ml k-casein and 0.1% methylcellulose, 5% sucrose), with an oxygen scavenger system [50 mM glucose, 400 mg/ml glucose oxidase, 200 mg/ml catalase and 4 mM dithiothreitol (DTT)] and 4 nM Klp67A-GFP, was flowed into the chamber. The single kinesin motility assay was conducted following other publications (Naito and Goshima, 2015) with slight modification to the buffer. A silanized coverslip was coated with anti-biotin antibody, and a solution containing 1% pluronic acid was loaded into the chamber. After washing once with 1 × MRB80, GMPCPP-stabilised MTs labelled with Alexa 647 and biotin were loaded. After a 1 × MRB80 wash, Klp67A-GFP was loaded into the chamber with a buffer identical to that used for the *in vitro* MT polymerisation assay.

Data analysis

MT attachment instability was determined by counting the detachment events over time (monotelic to unattachment/lateral interaction or syntelic to monotelic conversion), whereas MT attachment frequency was obtained for monotelically-attached chromosomes. MT plus-end dynamics *in vitro* were analysed based on kymographs, following others (Moriwaki and Goshima, 2016): catastrophe frequency was determined by dividing the number of shrinkage events by the sum of growth and pause times,

whereas the transition from shrinkage to pause or growth was considered a rescue event and the rescue frequency (for shrinkage time) was calculated. When MTs did not grow or shrink more than two pixels (0.32 μm) for five or more frames (15 s), this period was defined as a pause.

Acknowledgements
We thank Kosuke Ariga for helping data analysis and Tomomi Kiyomitsu for valuable comments on the manuscript. This work was funded by JSPS KAKENHI (15KT0077, 17H01431) to G.G. T.E. is a recipient of a JSPS pre-doctoral fellowship (16J02807). The authors declare no competing financial interests.

Author contributions
E.T. and G.G. conceived and designed the research project. E.T. performed the experiments and analysed the data. G.G. wrote the paper.

References

Al-Bassam, J., Kim, H., Brouhard, G., van Oijen, A., Harrison, S.C., and Chang, F. (2010). CLASP promotes microtubule rescue by recruiting tubulin dimers to the microtubule. Dev Cell **19,** 245-258.

Basto, R., Scaerou, F., Mische, S., Wojcik, E., Lefebvre, C., Gomes, R., Hays, T., and Karess, R. (2004). In vivo dynamics of the rough deal checkpoint protein during Drosophila mitosis. Curr Biol **14,** 56-61.

Bettencourt-Dias, M., and Goshima, G. (2009). RNAi in Drosophila S2 cells as a tool for studying cell cycle progression. Methods Mol Biol **545,** 39-62.

Buster, D.W., Zhang, D., and Sharp, D.J. (2007). Poleward tubulin flux in spindles: regulation and function in mitotic cells. Mol Biol Cell **18,** 3094-3104.

Cheeseman, I.M., Chappie, J.S., Wilson-Kubalek, E.M., and Desai, A. (2006). The conserved KMN network constitutes the core microtubule-binding site of the kinetochore. Cell **127,** 983-997.

Cheeseman, I.M., Anderson, S., Jwa, M., Green, E.M., Kang, J., Yates, J.R., 3rd, Chan, C.S., Drubin, D.G., and Barnes, G. (2002). Phospho-regulation of kinetochore-microtubule attachments by the Aurora kinase Ipl1p. Cell **111,** 163-172.

Cottingham, F.R., and Hoyt, M.A. (1997). Mitotic spindle positioning in Saccharomyces cerevisiae is accomplished by antagonistically acting microtubule motor proteins. J Cell Biol **138,** 1041-1053.

De Wever, V., Nasa, I., Chamousset, D., Lloyd, D., Nimick, M., Xu, H., Trinkle-Mulcahy, L., and Moorhead, G.B. (2014). The human mitotic kinesin KIF18A binds protein phosphatase 1 (PP1) through a highly conserved docking motif. Biochem Biophys Res Commun **453,** 432-437.

DeLuca, J.G., Gall, W.E., Ciferri, C., Cimini, D., Musacchio, A., and Salmon, E.D. (2006). Kinetochore microtubule dynamics and attachment stability are regulated by Hec1. Cell **127,** 969-982.

Du, Y., English, C.A., and Ohi, R. (2010). The kinesin-8 Kif18A dampens microtubule plus-end dynamics. Curr Biol **20,** 374-380.

Erent, M., Drummond, D.R., and Cross, R.A. (2012). S. pombe kinesins-8 promote both nucleation and catastrophe of microtubules. PLoS One **7,** e30738.

Gandhi, R., Bonaccorsi, S., Wentworth, D., Doxsey, S., Gatti, M., and Pereira, A. (2004). The Drosophila kinesin-like protein KLP67A is essential for mitotic and male meiotic spindle assembly. Mol Biol Cell **15,** 121-131.

Garcia, M.A., Vardy, L., Koonrugsa, N., and Toda, T. (2001). Fission yeast ch-TOG/XMAP215 homologue Alp14 connects mitotic spindles with the kinetochore and is a component of the Mad2-dependent spindle checkpoint. EMBO J **20,** 3389-3401.

Gatt, M.K., Savoian, M.S., Riparbelli, M.G., Massarelli, C., Callaini, G., and Glover, D.M. (2005). Klp67A destabilises pre-anaphase microtubules but subsequently is required to stabilise the central spindle. J Cell Sci **118,** 2671-2682.

Gluszek, A.A., Cullen, C.F., Li, W., Battaglia, R.A., Radford, S.J., Costa, M.F., McKim, K.S., Goshima, G., and Ohkura, H. (2015). The microtubule catastrophe promoter Sentin delays stable kinetochore-microtubule attachment in oocytes. J Cell Biol **211,** 1113-1120.

Goshima, G., and Vale, R.D. (2003). The roles of microtubule-based motor proteins in mitosis: comprehensive RNAi analysis in the Drosophila S2 cell line. J Cell Biol **162,** 1003-1016.

Goshima, G., and Vale, R.D. (2005). Cell cycle-dependent dynamics and regulation of mitotic kinesins in Drosophila S2 cells. Mol Biol Cell **16,** 3896-3907.

Goshima, G., Wollman, R., Stuurman, N., Scholey, J.M., and Vale, R.D. (2005). Length control of the metaphase spindle. Curr Biol **15,** 1979-1988.

Goshima, G., Mayer, M., Zhang, N., Stuurman,

N., and Vale, R.D. (2008). Augmin: a protein complex required for centrosome-independent microtubule generation within the spindle. J Cell Biol **181,** 421-429.

Goshima, G., Wollman, R., Goodwin, N., Zhang, J.M., Scholey, J.M., Vale, R.D., and Stuurman, N. (2007). Genes required for mitotic spindle assembly in Drosophila S2 cells. Science **316,** 417-421.

Gupta, M.L., Jr., Carvalho, P., Roof, D.M., and Pellman, D. (2006). Plus end-specific depolymerase activity of Kip3, a kinesin-8 protein, explains its role in positioning the yeast mitotic spindle. Nat Cell Biol **8,** 913-923.

Hitti, E., Bakheet, T., Al-Souhibani, N., Moghrabi, W., Al-Yahya, S., Al-Ghamdi, M., Al-Saif, M., Shoukri, M.M., Lanczky, A., Grepin, R., Gyorffy, B., Pages, G., and Khabar, K.S. (2016). Systematic Analysis of AU-Rich Element Expression in Cancer Reveals Common Functional Clusters Regulated by Key RNA-Binding Proteins. Cancer Res **76,** 4068-4080.

Ito, A., and Goshima, G. (2015). Microcephaly protein Asp focuses the minus ends of spindle microtubules at the pole and within the spindle. J Cell Biol **211,** 999-1009.

Kim, H., and Stumpff, J.K. (2018). Kif18A promotes Hec1 dephosphorylation to coordinate chromosome alignment with kinetochore microtubule attachment. bioRxiv **304147**.

Lampson, M.A., and Grishchuk, E.L. (2017). Mechanisms to Avoid and Correct Erroneous Kinetochore-Microtubule Attachments. Biology (Basel) **6**.

Li, W., Moriwaki, T., Tani, T., Watanabe, T., Kaibuchi, K., and Goshima, G. (2012). Reconstitution of dynamic microtubules with Drosophila XMAP215, EB1, and Sentin. J Cell Biol **199,** 849-862.

Locke, J., Joseph, A.P., Pena, A., Mockel, M.M., Mayer, T.U., Topf, M., and Moores, C.A. (2017). Structural basis of human kinesin-8 function and inhibition. Proc Natl Acad Sci U S A **114,** E9539-E9548.

Maiato, H., Khodjakov, A., and Rieder, C.L. (2005). Drosophila CLASP is required for the incorporation of microtubule subunits into fluxing kinetochore fibres. Nat Cell Biol **7,** 42-47.

Maiato, H., Fairley, E.A., Rieder, C.L., Swedlow, J.R., Sunkel, C.E., and Earnshaw, W.C. (2003). Human CLASP1 is an outer kinetochore component that regulates spindle microtubule dynamics. Cell **113,** 891-904.

Mayr, M.I., Storch, M., Howard, J., and Mayer, T.U. (2011). A non-motor microtubule binding site is essential for the high processivity and mitotic function of kinesin-8 Kif18A. PLoS One **6,** e27471.

Mayr, M.I., Hummer, S., Bormann, J., Gruner, T., Adio, S., Woehlke, G., and Mayer, T.U. (2007). The human kinesin Kif18A is a motile microtubule depolymerase essential for chromosome congression. Curr Biol **17,** 488-498.

McHugh, T., Gluszek, A.A., and Welburn, J.P.I. (2018). Microtubule end tethering of a processive kinesin-8 motor Kif18b is required for spindle positioning. J Cell Biol.

Miki, T., Nishina, M., and Goshima, G. (2015). RNAi screening identifies the armadillo repeat-containing kinesins responsible for microtubule-dependent nuclear positioning in Physcomitrella patens. Plant Cell Physiol **56,** 737-749.

Moriwaki, T., and Goshima, G. (2016). Five factors can reconstitute all three phases of microtubule polymerization dynamics. J Cell Biol **215,** 357-368.

Musacchio, A., and Desai, A. (2017). A Molecular View of Kinetochore Assembly and Function. Biology (Basel) **6**.

Naito, H., and Goshima, G. (2015). NACK kinesin is required for metaphase chromosome alignment and cytokinesis in the moss Physcomitrella patens. Cell Struct Funct **40,** 31-41.

Powers, A.F., Franck, A.D., Gestaut, D.R., Cooper, J., Gracyzk, B., Wei, R.R., Wordeman, L., Davis, T.N., and Asbury, C.L. (2009). The Ndc80 kinetochore complex forms load-bearing attachments to dynamic microtubule tips via biased diffusion. Cell **136,** 865-875.

Rogers, G.C., Rogers, S.L., Schwimmer, T.A., Ems-McClung, S.C., Walczak, C.E., Vale, R.D., Scholey, J.M., and Sharp, D.J. (2004). Two mitotic kinesins cooperate to drive sister chromatid separation during anaphase. Nature **427,** 364-370.

Savoian, M.S., and Glover, D.M. (2010). Drosophila Klp67A binds prophase kinetochores to subsequently regulate congression and spindle length. J Cell Sci **123,** 767-776.

Savoian, M.S., Gatt, M.K., Riparbelli, M.G., Callaini, G., and Glover, D.M. (2004). Drosophila Klp67A is required for proper chromosome congression and segregation during meiosis I. J Cell Sci **117,** 3669-3677.

Schmidt, J.C., Arthanari, H., Boeszoermenyi, A., Dashkevich, N.M., Wilson-Kubalek, E.M., Monnier, N., Markus, M., Oberer, M., Milligan, R.A., Bathe, M., Wagner, G., Grishchuk, E.L., and Cheeseman, I.M. (2012). The kinetochore-bound Ska1 complex

tracks depolymerizing microtubules and binds to curved protofilaments. Dev Cell **23,** 968-980.

Smurnyy, Y., Toms, A.V., Hickson, G.R., Eck, M.J., and Eggert, U.S. (2010). Binucleine 2, an isoform-specific inhibitor of Drosophila Aurora B kinase, provides insights into the mechanism of cytokinesis. ACS Chem Biol **5,** 1015-1020.

Straight, A.F., Sedat, J.W., and Murray, A.W. (1998). Time-lapse microscopy reveals unique roles for kinesins during anaphase in budding yeast. J Cell Biol **143,** 687-694.

Stumpff, J., von Dassow, G., Wagenbach, M., Asbury, C., and Wordeman, L. (2008). The kinesin-8 motor Kif18A suppresses kinetochore movements to control mitotic chromosome alignment. Dev Cell **14,** 252-262.

Stumpff, J., Du, Y., English, C.A., Maliga, Z., Wagenbach, M., Asbury, C.L., Wordeman, L., and Ohi, R. (2011). A tethering mechanism controls the processivity and kinetochore-microtubule plus-end enrichment of the kinesin-8 Kif18A. Mol Cell **43,** 764-775.

Su, X., Qiu, W., Gupta, M.L., Jr., Pereira-Leal, J.B., Reck-Peterson, S.L., and Pellman, D. (2011). Mechanisms underlying the dual-mode regulation of microtubule dynamics by Kip3/kinesin-8. Mol Cell **43,** 751-763.

Su, X., Arellano-Santoyo, H., Portran, D., Gaillard, J., Vantard, M., Thery, M., and Pellman, D. (2013). Microtubule-sliding activity of a kinesin-8 promotes spindle assembly and spindle-length control. Nat Cell Biol **15,** 948-957.

Tien, J.F., Umbreit, N.T., Gestaut, D.R., Franck, A.D., Cooper, J., Wordeman, L., Gonen, T., Asbury, C.L., and Davis, T.N. (2010). Cooperation of the Dam1 and Ndc80 kinetochore complexes enhances microtubule coupling and is regulated by aurora B. J Cell Biol **189,** 713-723.

Tytell, J.D., and Sorger, P.K. (2006). Analysis of kinesin motor function at budding yeast kinetochores. J Cell Biol **172,** 861-874.

Varga, V., Helenius, J., Tanaka, K., Hyman, A.A., Tanaka, T.U., and Howard, J. (2006). Yeast kinesin-8 depolymerizes microtubules in a length-dependent manner. Nat Cell Biol **8,** 957-962.

Wang, H., Brust-Mascher, I., Cheerambathur, D., and Scholey, J.M. (2010). Coupling between microtubule sliding, plus-end growth and spindle length revealed by kinesin-8 depletion. Cytoskeleton (Hoboken) **67,** 715-728.

Wargacki, M.M., Tay, J.C., Muller, E.G., Asbury, C.L., and Davis, T.N. (2010). Kip3, the yeast kinesin-8, is required for clustering of kinetochores at metaphase. Cell Cycle **9,** 2581-2588.

Weaver, L.N., Ems-McClung, S.C., Stout, J.R., LeBlanc, C., Shaw, S.L., Gardner, M.K., and Walczak, C.E. (2011). Kif18A uses a microtubule binding site in the tail for plus-end localization and spindle length regulation. Curr Biol **21,** 1500-1506.

West, R.R., Malmstrom, T., and McIntosh, J.R. (2002). Kinesins klp5(+) and klp6(+) are required for normal chromosome movement in mitosis. J Cell Sci **115,** 931-940.

Widlund, P.O., Podolski, M., Reber, S., Alper, J., Storch, M., Hyman, A.A., Howard, J., and Drechsel, D.N. (2012). One-step purification of assembly-competent tubulin from diverse eukaryotic sources. Mol Biol Cell **23,** 4393-4401.

Yu, N., Signorile, L., Basu, S., Ottema, S., Lebbink, J.H., Leslie, K., Smal, I., Dekkers, D., Demmers, J., and Galjart, N. (2016). Isolation of functional tubulin dimers and of tubulin-associated proteins from mammalian cells. Curr Biol **26,** 1728-1736.

Zhang, C., Zhu, C., Chen, H., Li, L., Guo, L., Jiang, W., and Lu, S.H. (2010). Kif18A is involved in human breast carcinogenesis. Carcinogenesis **31,** 1676-1684.

Table S1. Plasmids used in this study

Name	Insert	Vector	Note
pED128	Klp67A-GFP -6His	pET23	
pGG952	6His-Klp10A	pDES T17	Moriw aki and Goshi ma (2016)
pED158	sfGFP-Rod	pAc	
pGFP-CLA SP	GFP-Mast/O rbit	pMT	Goshi ma et al. (2007)
pGG482	H2B-mCherr y	pAc	
pCoHygro mycin	HygR	Copia	

Supplemental Movie Legends

Movie 1. MT attachment stability in the monopolar spindle in the presence or absence of kinesin-8^{Klp67A}
GFP-Rod (green), H2B-mCherry (blue), and SiR-tubulin (magenta) images were acquired every 3 s with spinning-disc confocal microscopy in kinesin-5^{Klp61F} single or kinesin-8^{Klp67A}/kinesin-5^{Klp61F} double RNAi-treated cells. Bar, 5 μm.

Movie 2. MT attachment stability in the bipolar spindle in the presence or absence of kinesin-8^{Klp67A}
GFP-Rod (green), H2B-mCherry (blue), and SiR-tubulin (magenta) images were acquired every 3 s with spinning-disc confocal microscopy in kinesin-8^{Klp67A} or control RNAi-treated cells. Bar, 5 μm.

Movie 3. MT attachment stability in the absence of augmin^{Dgt6}
GFP-Rod (green), H2B-mCherry (blue), and SiR-tubulin (magenta) images were acquired every 3 s with spinning-disc confocal microscopy in augmin^{Dgt6}/kinesin-5^{Klp61F} RNAi-treated cells. Bar, 5 μm.

Movie 4. Stable syntelic attachment in the monopolar spindle after Aurora B inhibition in the absence of kinesin-8^{Klp67A}
GFP-Rod (green), H2B-mCherry (blue), and SiR-tubulin (magenta) images were acquired every 3 s with spinning-disc confocal microscopy in augmin^{Dgt6}/kinesin-5^{Klp61F} RNAi-treated cells. Twenty μM Binucleine 2 (*Drosophila* Aurora B inhibitor) was added at time 0. Bar, 5 μm.

Movie 5. CLASP$^{Mast/Orbit}$ overexpression rescued MT attachment stability in the absence of kinesin-8^{Klp67A}
GFP-Rod and GFP-CLASP$^{Mast/Orbit}$ (green), H2B-mCherry (blue), and SiR-tubulin (magenta) images were acquired every 3 s with spinning-disc confocal microscopy in kinesin-8^{Klp67A}/kinesin-5^{Klp61F} double RNAi-treated cells expressing GFP-CLASP$^{Mast/Orbit}$. Bar, 5 μm.

Figure 1

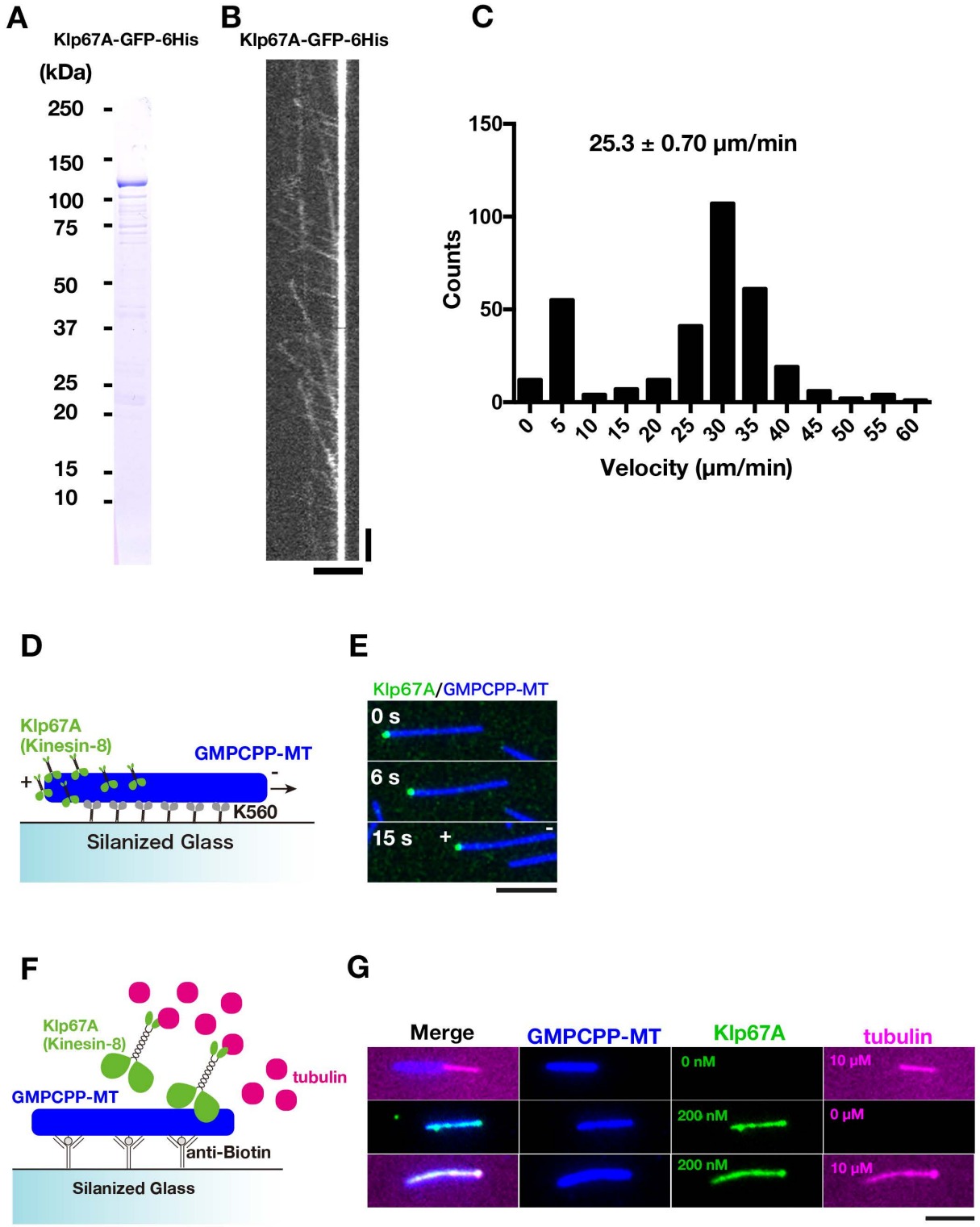

Figure 1. Kinesin-8^{Klp67A} is a processive plus-end-directed motor which can bind to tubulin
(A) Coomassie staining of purified, full-length kinesin-8^{Klp67A} tagged with GFP and 6 x His. **(B)** Kymograph showing processive motility of kinesin-8^{Klp67A}-GFP (100 pM) along MTs and accumulation at the MT end. Each punctate signal represents a single kinesin-8^{Klp67A}-GFP dimer, based on the signal intensity. Horizontal bar, 5 µm; Vertical bar, 20 s. **(C)** Plot of kinesin-8^{Klp67A}-GFP run velocity, calculated based on kymographs (n = 331). Immobile GFP signals were not counted (the "0" column represents velocity between 0 and 5 µm/min). **(D, E)** Gliding of stabilised MTs (blue) by the plus-end-directed human kinesin-1 motor (K560 construct; non-fluorescent). Rightward motility of MTs indicate that the left end corresponds to MT plus end. Kinesin-8^{Klp67A}-GFP (green, 4 nM) accumulated specifically at the plus end. **(F, G)** Tubulin recruitment by kinesin-8Klp67A. Tubulin (10 µM, magenta) and kinesin-8^{Klp67A} (green; 0.2 µM), which bound to GMPCPP-stabilised MTs (blue), were mixed, and tubulin localisation along MTs was investigated. Bar, 5 µm.

Figure 2

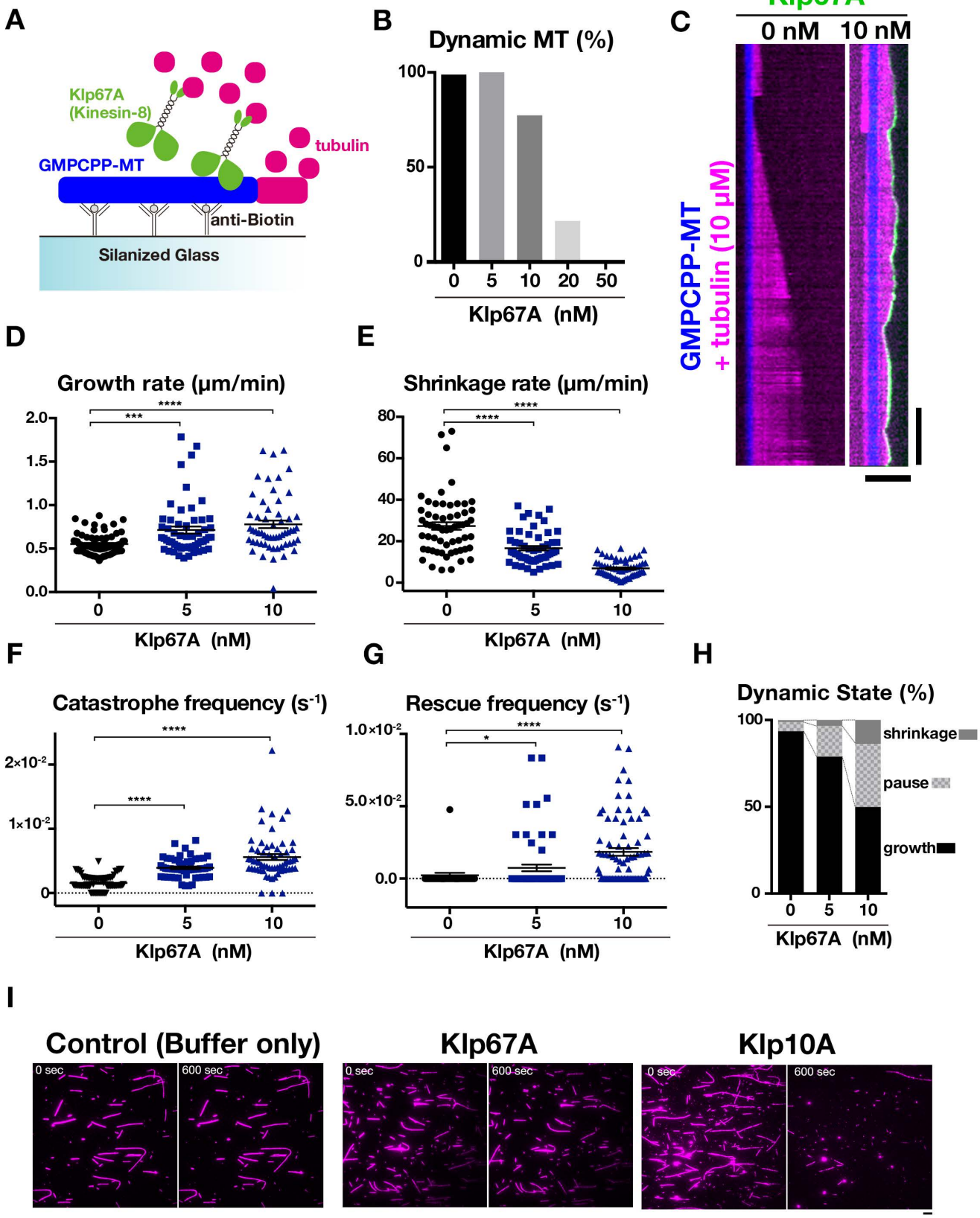

Figure 2. Kinesin-8^{Klp67A} regulates MT plus-end dynamics in vitro

(A) Schematic presentation of the in vitro MT polymerisation assay. **(B)** Inhibitory effect of kinesin-8^{Klp67A} on MT polymerisation from the seed (n = 84, 74, 84, 74, 94 from left to right). **(C)** MT dynamics are represented by kymographs. MTs stabilised with GMPCPP are coloured blue, dynamics MTs are magenta, and kinesin-8^{Klp67A}-GFP (0 or 10 nM) is green. Horizontal bar, 5 μm; Vertical bar, 120 s. **(D–H)** Parameters of MT plus end dynamics. Experiments were performed twice and the combined data are displayed (the change in rate/frequency by kinesin-8^{Klp67A} was reproduced). N = 41 + 33 (0 nM), 25 + 31 (5 nM), 20 + 41 (10 nM). Each dot represents a value obtained from a single MT and error bars represent SEM. Note that rescue was rarely observed in the absence of kinesin-8^{Klp67A}. $p < 0.0001$ (****), $p < 0.002$ (***), or $p < 0.03$ (*) by Games-Howell (D–F) or Steel Dwass (G) tests. **(I)** Kinesin-8^{Klp67A} (10 nM) cannot depolymerise GMPCPP-stabilised MTs. MTs stabilised with GMPCPP were mixed with full-length kinesin-8^{Klp67A} (10 nM) and, as a positive control, MT depolymerase kinesin-13^{Klp10A} (10 nM). Bar, 5 μm.

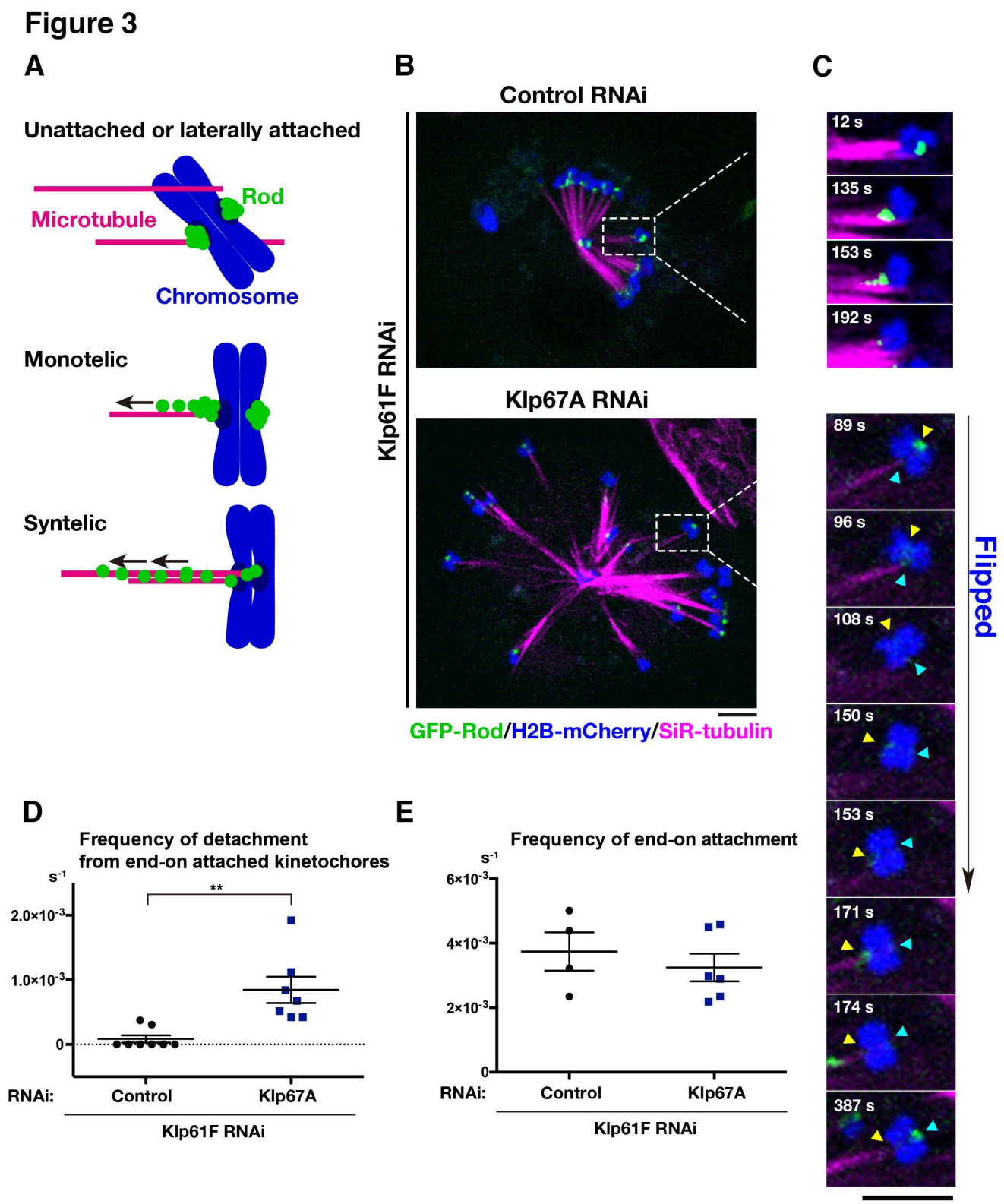

Figure 3. Kinesin-8^{Klp67A} is required for stable kinetochore-MT attachment: monopolar spindle
(A) Diagram of GFP-Rod and MT attachment mode. **(B)** Monopolar spindles formed after RNAi of kinesin-5^{Klp61F} (top) or double kinesin-5^{Klp61F}/ kinesin-8^{Klp67A} (bottom). Blue, chromosome (H2B-mCherry); Green, GFP-Rod; Magenta, MT (SiR-tubulin). **(C)** (Top) Monotelic-to-syntelic conversion in the control monopolar spindle; upon new MT association, GFP-Rod flux was observed along the kinetochore MT (153 s), and subsequently, the GFP signal diminished at the kinetochore (192 s). (Bottom) Chromosome flipping was observed in the absence of kinesin-8^{Klp67A} (89–171 s; sister kinetochores are indicated by yellow and blue arrows). **(D)** Increased frequency (event # per chromosome per sec) of MT detachment in the absence of kinesin-8^{Klp67A} ($p < 0.009$, Welch's t-test). Events were counted when MTs terminated end-on attachment. RNAi and imaging were performed four times, data were quantitatively analysed twice, and the two datasets were combined. Each dot in the graph represents mean frequency for a cell. A total of 86 chromosomes in 8 cells (control) and 56 chromosomes in 8 cells (kinesin-8^{Klp67A} RNAi) were analysed. **(E)** Frequency (event # per chromosome per sec) of newly acquired end-on attachment that was indicated by GFP-Rod flux along kinetochore MTs. The attachment number was divided by the total time the chromosomes spent in a monotelic or unattached state. Each dot in the graph represents mean frequency for a cell. A total of 18 chromosomes in 4 cells (control) and 18 chromosomes in 6 cells (kinesin-8^{Klp67A} RNAi) were analysed. Error bars indicate SEM. Bars, 5 μm.

Figure 4

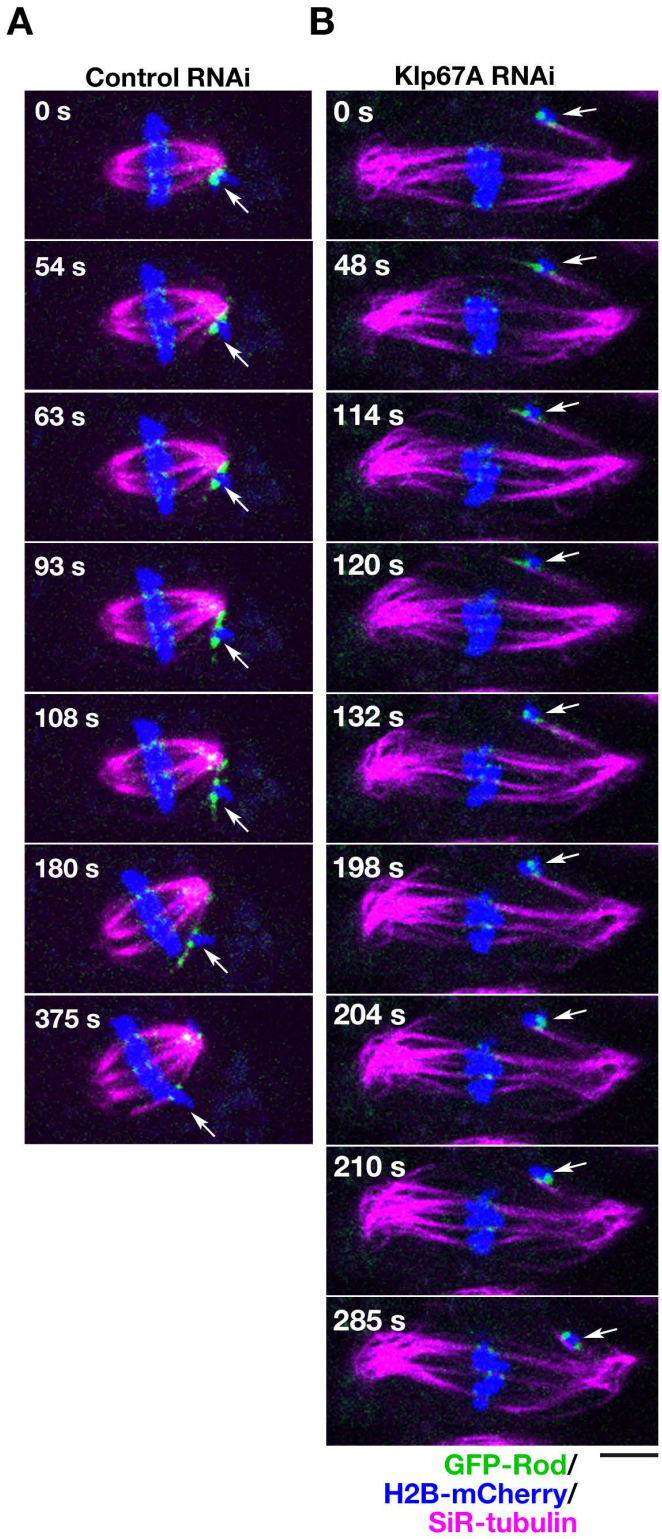

Figure 4. Kinesin-8^{Klp67A} is required for stable kinetochore-MT attachment: bipolar spindle
(A, B) Time-lapse imaging of spindle MTs (magenta; SiR-tubulin staining), chromosomes (blue; H2B-mCherry), and GFP-Rod (green) after control or kinesin-8^{Klp67A} RNAi. The behaviour of an initially unaligned chromosome (arrow) was dramatically different. Bar, 5 μm.

Figure 5

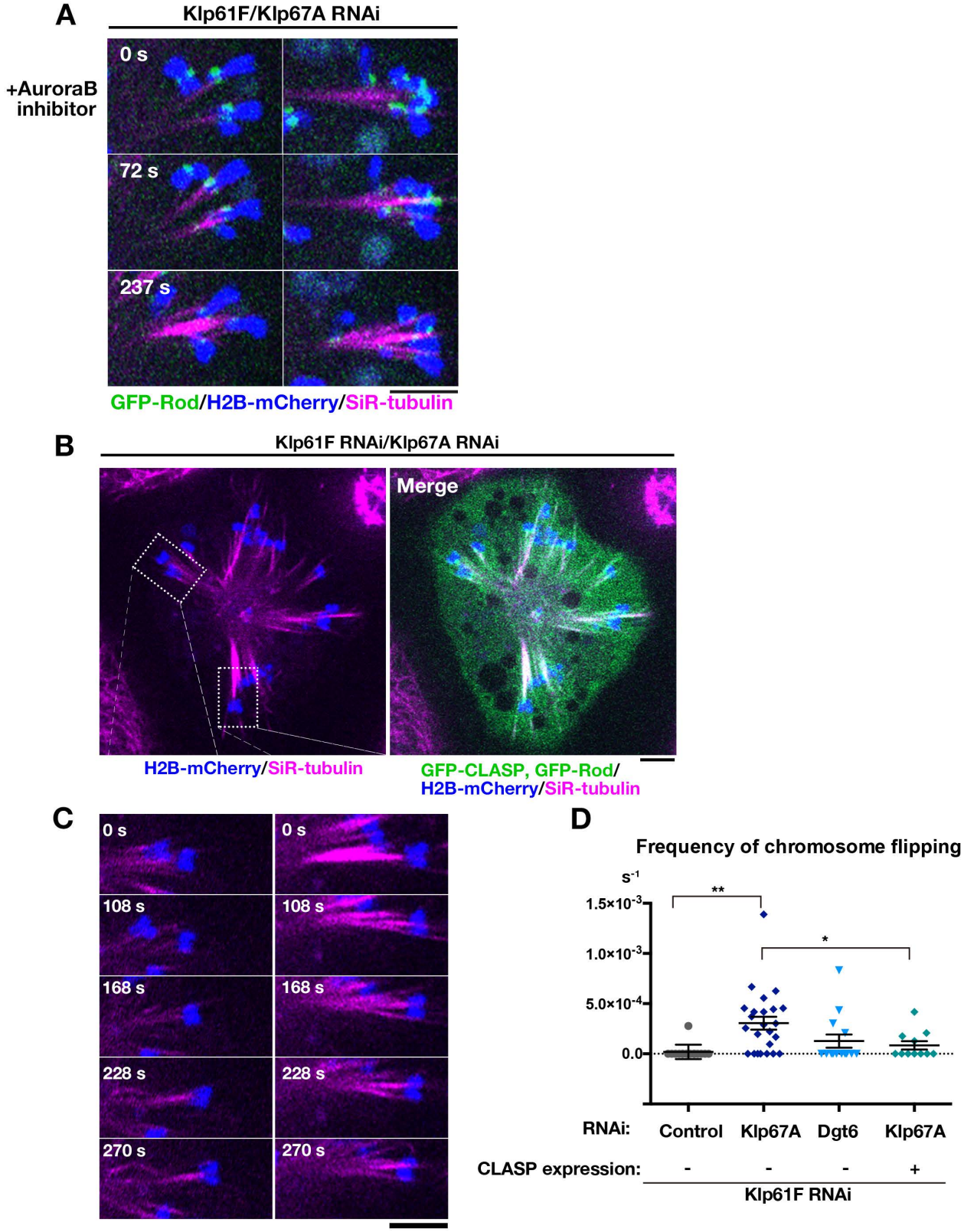

Figure 5. MT attachment stability was restored by inhibiting Aurora B kinase or CLASP$^{Mast/Orbit}$ overexpression
(A) Monopolar spindles treated with 20 μM Binucleine-2, an inhibitor of Drosophila Aurora B kinase. Spindles after kinesin-5^{Klp61F} RNAi (left) and after double kinesin-5^{Klp61F}/kinesin-8^{Klp67A} RNAi (right) are presented. **(B)** GFP-CLASP$^{Mast/Orbit}$ overexpression in the monopolar spindle depleted of kinesin-5^{Klp61F} and kinesin-8$^{Klp67A.}$ **(C)** Two representative chromosomes (inset in B). Chromosomes were static when GFP-CLASP$^{Mast/Orbit}$ was overexpressed. **(D)** Frequency of chromosome flipping (per chromosome, per sec). Expression of GFP-CLASP$^{Mast/Orbit}$ significantly reduced the frequency of flipped chromosomes (**$p < 0.0013$, *$p < 0.034$, Games-Howell test). RNAi (and overexpression) were performed two or more times, and combined data are presented. Each dot in the graph represents mean frequency for a cell. A total of 168 chromosomes in 15 cells (control), 364 chromosomes in 24 cells (kinesin-8^{Klp67A} RNAi), 128 chromosomes in 13 cells (augmin^{Dgt6} RNAi), 128 chromosomes in 11 cells (kinesin-8^{Klp67A} RNAi and GFP-CLASP$^{Mast/Orbit}$ overexpression) were analysed. Bars, 5 μm.

FigureS1

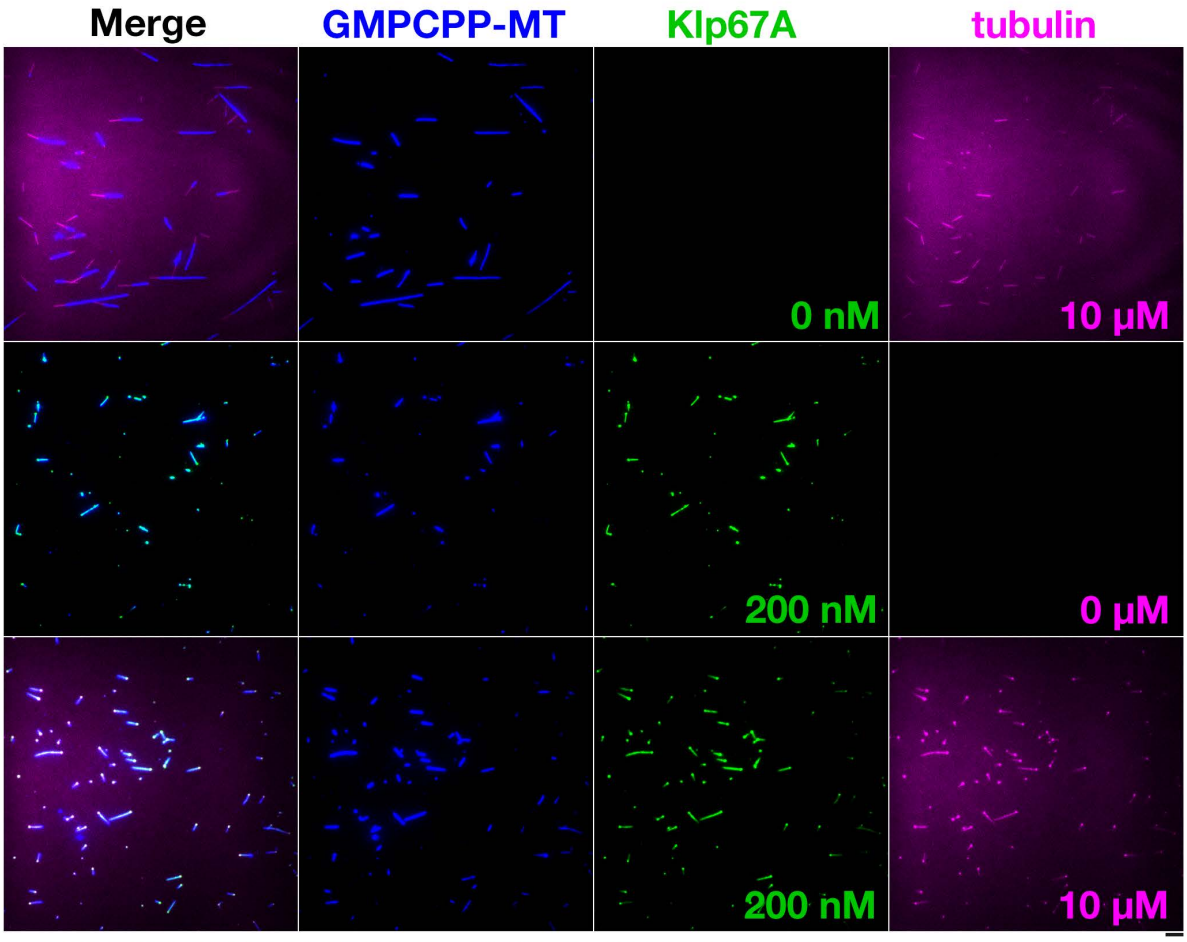

Figure S1. Tubulin-binding activity of kinesin-8^{Klp67A} (more examples of Fig. 1G)
Tubulin recruitment by kinesin-8^{Klp67A}. Tubulin (10 μM, magenta) and kinesin-8^{Klp67A} (green; 0.2 μM), which bound to GMPCPP-stabilised MTs (blue), were mixed, and tubulin localisation along MTs was investigated. Bar, 5 μm.

Figure S2

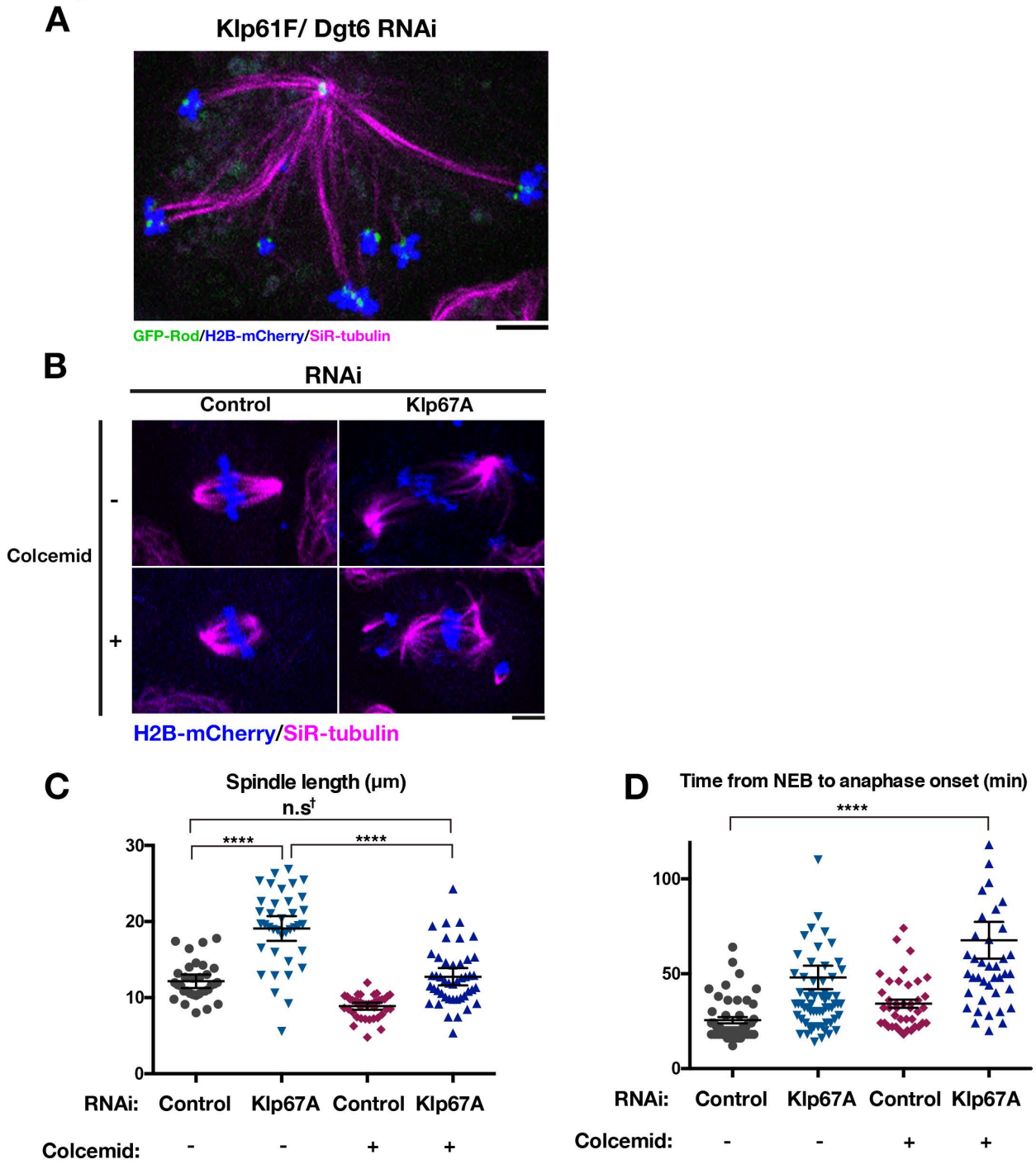

Figure S2. Artificial MT shortening cannot rescue chromosome misalignment induced by kinesin-8^{Klp67A} depletion
(A) Elongated monopolar spindle after double RNAi knockdown of augmin^{Dgt6} and kinesin-5^{Klp61F}. GFP-Rod signals indicated the presence of both monotelic and syntelic chromosomes. See Movie 3 for chromosome/kinetochore dynamics. **(B–D)** Force-shortening of the spindle by colcemid treatment (60 ng/mL) in kinesin-8^{Klp67A} RNAi-treated cells did not recover chromosome misalignment **(B)** and mitotic progression **(D)**, despite that the spindle was shortened to the control level **(C)**. Spindle length was measured at 16 min after NEBD. Marked with † is the comparison between control RNAi and kinesin-8^{Klp67A} RNAi + colcemid: mean difference = 0.59, 95 % confidence interval on the difference = [-1.28, 2.46]. **** indicates significant ($p < 0.001$) difference by Games-Howell test. N = 33, 38, 45 and 40 (C; from left to right), and 46, 66, 40, 41 (D, from left to right). Error bars indicate SEM. Experiments were performed twice, and the data from one experiment is presented. Two outliers obtained in kinesin-8^{Klp67A} RNAi-treated cells in (D) are not described in the graph but were taken into account during mean and SEM calculations. Bars, 5 µm.